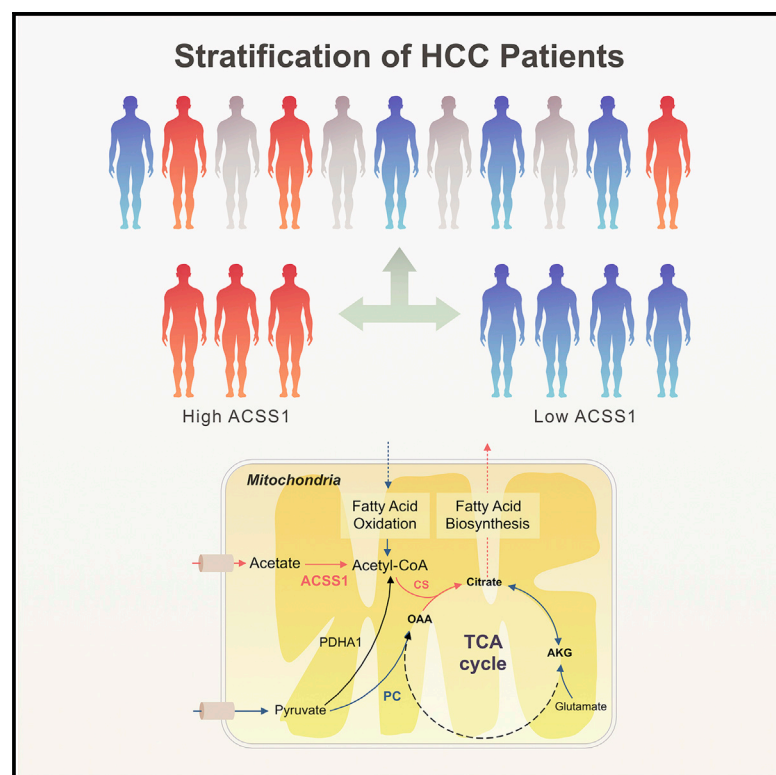# Cell Reports

Stratification of Hepatocellular Carcinoma Patients Based on Acetate Utilization

Graphical Abstract

Authors

Elias Björnson, Bani Mukhopadhyay, Anna Asplund, ..., George Kunos, Jens Nielsen, Adil Mardinoglu

Correspondence

adilm@scilifelab.se

In Brief

Stratification of HCC patients is vital for the development of effective treatment strategies. Björnson et al. stratify HCC patients based on acetate utilization and find that mitochondrial acetate is a metabolic fuel under hypoxic conditions. This is mediated by ACSS1, which may be a potential therapeutic target for treatment of HCC.

Highlights

- Reconstruction of a genome-scale metabolic model for HCC tumors

- Revealing metabolic alterations in HCC

- Analysis of the heterogeneous expression of ACSS1 and ACSS2 between HCC tumors

- Induction of ACSS1 in murine and human HCC samples under hypoxic conditions

CrossMark

CellPress

Resource

Stratification of Hepatocellular Carcinoma Patients Based on Acetate Utilization

Elias Björnson,[1,9] Bani Mukhopadhyay,[2,9] Anna Asplund,[3,9] Nusa Pristovsek,[3] Resat Cinar,[2] Stefano Romeo,[4,5,6] Mathias Uhlen,[7,8] George Kunos,[2] Jens Nielsen,[1,8] and Adil Mardinoglu[1,8,*]

[1]Department of Biology and Biological Engineering, Chalmers University of Technology, 412 96 Gothenburg, Sweden
[2]Laboratory of Physiologic Studies, National Institute on Alcohol Abuse and Alcoholism, National Institutes of Health, Bethesda, MD 20892, USA
[3]Department of Immunology, Genetics and Pathology, Science for Life Laboratory, Uppsala University, 751 85 Uppsala, Sweden
[4]Department of Molecular and Clinical Medicine, the Sahlgrenska Center for Cardiovascular and Metabolic Research/Wallenberg Laboratory, University of Gothenburg, 413 45 Gothenburg, Sweden
[5]Cardiology Department, Sahlgrenska University Hospital, 416 50 Gothenburg, Sweden
[6]Clinical Nutrition Unit, Department of Medical and Surgical Sciences, University Magna Graecia, 88100 Catanzaro, Italy
[7]Department of Proteomics, KTH-Royal Institute of Technology, 106 91 Stockholm, Sweden
[8]Science for Life Laboratory, KTH-Royal Institute of Technology, 171 21 Stockholm, Sweden
[9]Co-first author
*Correspondence: adilm@scilifelab.se
http://dx.doi.org/10.1016/j.celrep.2015.10.045

SUMMARY

Hepatocellular carcinoma (HCC) is a deadly form of liver cancer that is increasingly prevalent. We analyzed global gene expression profiling of 361 HCC tumors and 49 adjacent noncancerous liver samples by means of combinatorial network-based analysis. We investigated the correlation between transcriptome and proteome of HCC and reconstructed a functional genome-scale metabolic model (GEM) for HCC. We identified fundamental metabolic processes required for cell proliferation using the network centric view provided by the GEM. Our analysis revealed tight regulation of fatty acid biosynthesis (FAB) and highly significant deregulation of fatty acid oxidation in HCC. We predicted mitochondrial acetate as an emerging substrate for FAB through upregulation of mitochondrial acetyl-CoA synthetase (ACSS1) in HCC. We analyzed heterogeneous expression of ACSS1 and ACSS2 between HCC patients stratified by high and low ACSS1 and ACSS2 expression and revealed that ACSS1 is associated with tumor growth and malignancy under hypoxic conditions in human HCC.

INTRODUCTION

Hepatocellular carcinoma (HCC) is a deadly form of liver cancer, and it is currently the second leading cause of cancer-related deaths worldwide (European Association For The Study Of The Liver; European Organisation For Research And Treatment Of Cancer, 2012). Despite a number of available treatment strategies, the survival rate for HCC patients is low (Llovet et al.,

2008). Considering its rising prevalence, more targeted and effective treatment strategies are highly desirable for HCC.

Cancer development involves major metabolic alterations (Carracedo et al., 2013), and the complexity of metabolism has been captured by the reconstruction of genome-scale metabolic models (GEMs) (Lewis and Abdel-Haleem, 2013; Mardinoglu and Nielsen, 2015; O'Brien et al., 2015; Yizhak et al., 2015), one of the denominators in systems biology, to identify selective anti-cancer drug targets (Agren et al., 2014; Folger et al., 2011). A GEM is the collection of all known biochemical reactions occurring in a given healthy cell or cancer, and each of these reactions is associated with gene products catalyzing these reactions (Mardinoglu et al., 2013a, 2015; Mardinoglu and Nielsen, 2012; Oberhardt et al., 2013; Shoaie and Nielsen, 2014). To unveil the molecular mechanisms underlying cancer, cancer-specific GEMs have been reconstructed (Agren et al., 2012; Gatto et al., 2014; Ghaffari et al., 2015; Mardinoglu et al., 2013b; Yizhak et al., 2014).

Availability of GEMs together with the high-throughput data and methods of data analysis may enable increased understanding of the altered metabolism in cancer. In addition, differential expression (DE) and differential rank conservation (DIRAC) analysis (Eddy et al., 2010) extract different types of information from gene expression data and may complement each other. Here, we identified metabolic differences between 361 HCC tumors and 49 adjacent noncancerous liver tissue samples using global gene expression profiling (RNA sequencing [RNA-seq] data). We reconstructed a population-based functional GEM for HCC tumors by integrating the transcriptome and proteome of HCC and examined the changes in the gene expression data using DE and DIRAC analysis based on the network topology provided by the GEM. We performed DIRAC analysis to identify and measure network-level perturbations based on the relative levels of expression for participating genes (Figure S1; Supplemental Experimental Procedures). Finally, we discovered
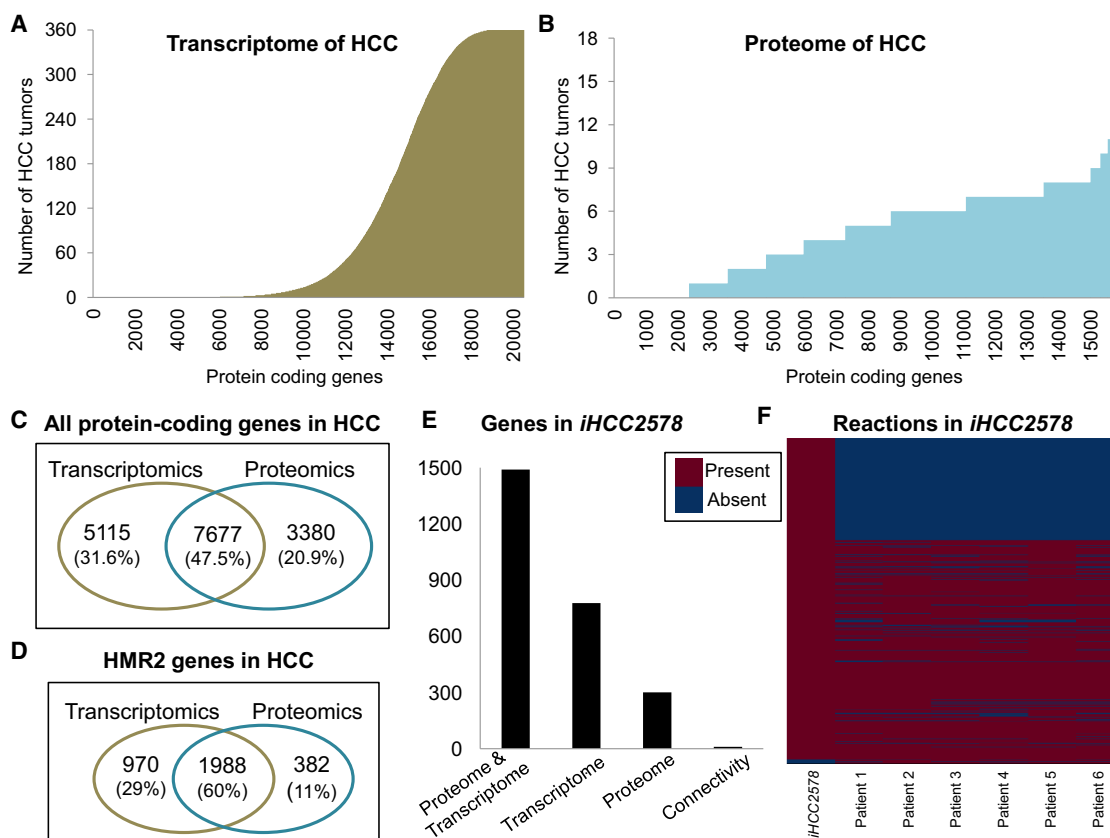
Figure 1. Reconstruction of the Functional GEM for HCC Tumor

(A and B) A functional generic GEM for HCC, *iHCC2578* is reconstructed based on transcriptome (A) and proteome (B) of the HCC tumors. The distributions of expression for the protein coding genes are illustrated based on transcriptome (A) and proteome (B) of HCC.

(C and D) All protein coding genes (C) and HMR2 genes (D) that are evaluated as present in HCC based on either in transcriptomics and proteomics data are used during the reconstruction of the *iHCC2578*.

(E) The source of evidence for the protein coding genes as well as the associated reactions incorporated into the model is shown.

(F) The content of *iHCC2578* is compared with the previously published personalized HCC models that are reconstructed based on proteomics data. *iHCC2578* contains all reactions in the personalized GEMs that are included based on HCC proteome.

See also Data S1.

heterogeneous expression of the acetate utilizing enzymes mitochondrial and cytosolic acetyl-CoA synthetase (ACSS1) and (ACSS2), respectively, within the HCC patients and compared the metabolic differences between HCC patients stratified by high and low ACSS1 and ACSS2 expression.

RESULTS

Defining HCC Proteome

We retrieved RNA-seq data for 361 individuals suffering from HCC as well as 49 noncancerous liver samples from The Cancer Genome Atlas database (TCGA). Based on mRNA expression data in TCGA, we interpreted low-abundance transcripts (transcripts per million [TPM] <10) as not being translated to their corresponding proteins based on our previous correlation analysis of transcriptome and proteome (Fagerberg et al., 2014; Väremo et al., 2015). We identified 12,792 (62%) of all putative protein coding genes (20,531) as being expressed in at least three of the 361 analyzed HCC tumors (Figure 1A; Data S1A). Recently,

we presented antibody-based proteome analysis of HCC tumors obtained from 27 male and female subjects (Agren et al., 2014) using the antibodies developed in Human Protein Atlas (HPA) (http://www.proteinatlas.org) (Kampf et al., 2014a, 2014b; Uhlén et al., 2015) and hereby identified 11,057 (70%) of the analyzed 15,841 proteins as being present in at least three of the HCC tumors (Figure 1B; Data S1B). Triplicate evaluations of every protein and transcript in HCC tumors were performed to avoid errors in experimental measurements during the identification of the HCC proteome and transcriptome. From comparison of two datasets, we found that 7,677 of the all protein coding genes (Figure 1C) and 1,988 of the protein coding genes in HMR2 (Mardinoglu et al., 2014) (Figure 1D) were consistently present in HCC. The differences between the coverage of the protein coding genes in HCC by transcriptome and proteome can be partly explained by the individual variations between the analyzed HCC tumors. Our findings were consistent with our previous study, where we analyzed the protein expression of six HCC patients and observed large variations between the HCC tumors (Agren

et al., 2014). However, such variations can cause limitations while performing DE analysis to detect altered biological processes in HCC compared to noncancerous liver, and we therefore reconstruct a consensus GEM for HCC that contains all possible metabolic reactions expressed in HCC tumors.

Generating a Functional Model for HCC, *iHCC2578*
In order to study the individual variations between HCC tumors, we performed network-dependent analysis using DIRAC based on the same metabolic network topology. In this context, we reconstructed a population-based functional GEM for HCC tumors, *iHCC2578*, using proteome and transcriptome of HCC. The 56 biological tasks (Data S1C) that represent the common metabolic functions known to occur in all human cells (e.g., synthesis of cholesterol) as well as the biological task for biomass growth were complemented to the tINIT algorithm together with the proteome and transcriptome of HCC. After manual evaluation, the resulting model includes 7,780 reactions, 2,578 associated genes to those reactions, and 5,584 metabolites in eight different subcellular compartments. The functionality of the *iHCC2578* was also tested successfully if the model can perform large number of (256) biological tasks that represent the major metabolic functions that occur in human metabolism (Data S1D).

The reconstructed model covers individual variations in HCC metabolism if detected in at least three of analyzed HCC tumors. Genes were incorporated into the model if they showed presence in HCC tumors based on proteome and transcriptome. The source of evidence for incorporation of the genes and associated reactions are shown in Figure 1E. We observed that only ten genes were included into the model due to the connectivity of the network, since we had evidence for all putative protein coding genes based on the transcriptome. We compared the content of *iHCC2578* with the six personalized HCC GEMs that have been reconstructed based on proteomics data (Agren et al., 2014) and found that *iHCC2578* contains 5,307 (98%) of the 5,405 reactions shared across all six personalized GEMs as well as 2,470 additional biochemical reactions (Figure 1F). We also investigated the reason for not incorporating the remaining 98 reactions in *iHCC2578* and found that those 98 reactions belonging to the personalized GEMs have been included into models due to the connectivity of the networks.

Distinct Differential Gene Expression Profile in HCC
To reveal the global biological differences between HCC tumors and noncancerous liver, we first identified differentially expressed genes (q value < 0.05) and hereby found 5,946 regulated genes (of 20,528) using differential expression sequencing (DESeq) (Data S1E). In order to gain more insights about the altered biological processes in HCC compared to noncancerous liver, we performed gene set analysis (GSA) for gene ontology (GO) biological process terms using PIANO R package (Väremo et al., 2013). We found that gene sets including DNA replication, DNA metabolic process, mitosis, and cell cycle are associated with upregulated genes, whereas catabolic processes and immune response are associated with downregulated genes in HCC (Figure S2).

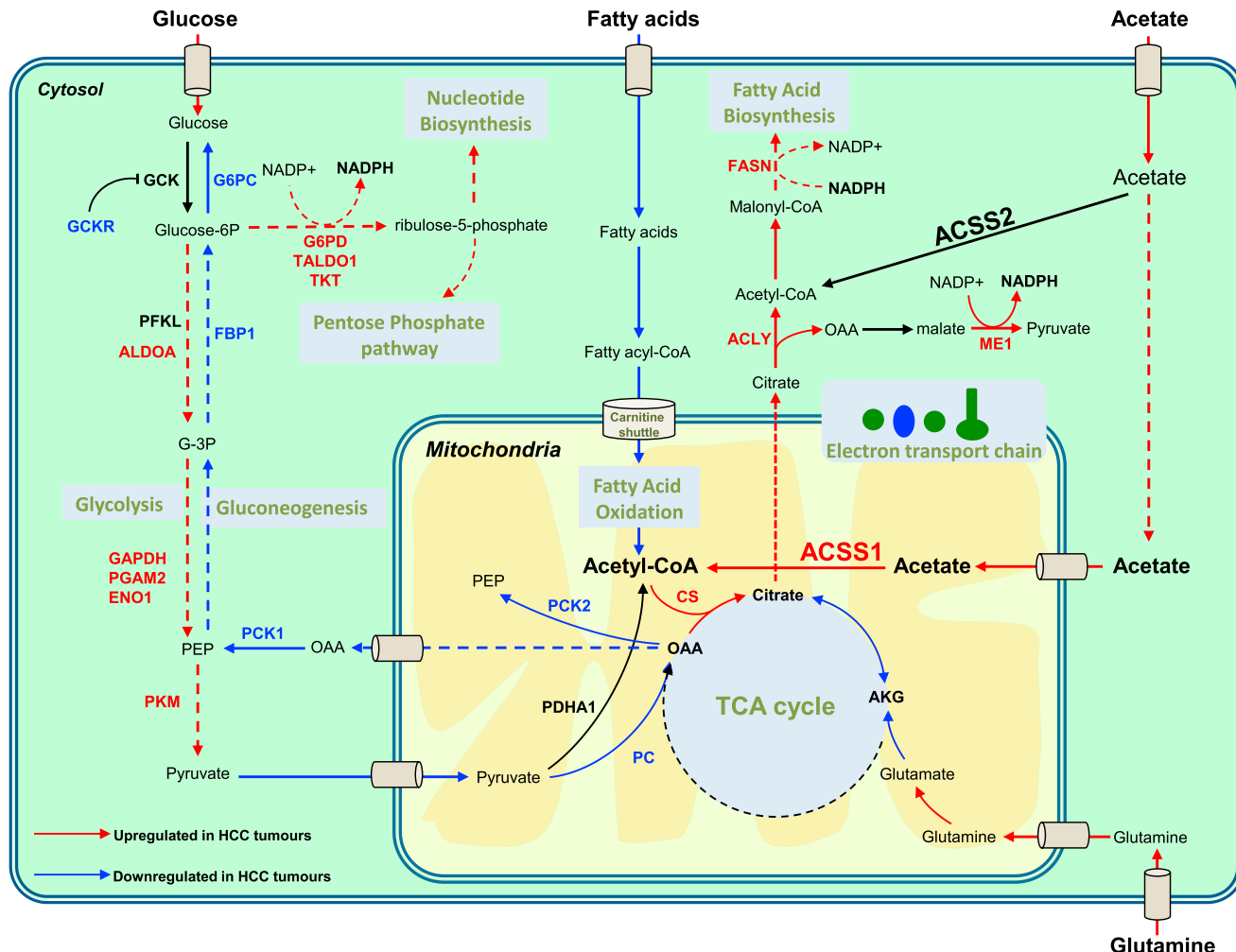We identified reporter metabolites for revealing the alterations in metabolism using the network structure provided by *iHCC2578*. The reporter metabolites algorithm has been developed to detect hotspot of the metabolism associated with up or downregulated genes between two phenotypes (Patil and Nielsen, 2005). We found that metabolites involved in histone and DNA methylation, lysine metabolism, l-carnitine synthesis, and tumor growth are associated with upregulated genes in HCC. Notably, oxygen was identified as a top reporter metabolite associated with the downregulated genes in HCC suggesting that oxygen is pivotal. (Figure S3; Data S1F).

In order to find tightly regulated and deregulated parts of the metabolism in HCC, we performed DIRAC analysis on the normalized gene expression data using the subsystems in *iHCC2578*. DIRAC analysis enabled identification of metabolic pathways reprogrammed differently in HCC patients and we predicted a high degree of deregulation of central metabolic pathways such as the tricarboxylic acid (TCA) cycle, electron transport chain (ETC), and fatty acid oxidation (FAO). In contrast, fatty acid biosynthesis (FAB) displayed tight regulation as defined by high conservation of transcript ordering in HCC, a rare occurrence since the vast majority of the metabolic pathways in cancer display some degree of deregulation. Figure 2 illustrates a summary of the alterations in major metabolic pathways in *iHCC2578* based on DE and DIRAC analysis. The fold changes and q values of the genes involved in each metabolic pathway, from the differential expression analysis are presented in Data S1G.

Increased De Novo Lipogenesis in HCC
The DIRAC analysis revealed FAB as one of the most tightly regulated pathways in HCC compared to noncancerous liver. This indicates that the expression of the genes involved in FAB showed similar reprogramming in all HCC patients. The DE analysis also pointed out significant (q value < 0.05) upregulation of key genes involved in FAB, including fatty acid synthase (FASN) in HCC tumors. In addition, citrate synthase (CS), which generates citrate from acetyl-CoA in mitochondria as well as ATP citrate lyase (ACLY), which in turn converts citrate to acetyl-CoA in the cytosol were significantly (q value < 0.05) upregulated. Key enzymes involved in FAB as well as enzymes catalyzing its preliminary step were upregulated in HCC indicating that FAB plays a major role in the proliferation of all HCC tumors.

In growing cells, there is an increased demand for NADPH to supply reducing equivalents required for biosynthetic processes. NADPH required for FAB can be produced through the conversion of malate to pyruvate in the cytosol by malic enzyme 1 (ME1) and in the pentose phosphate (PP) pathway. Notably, we found that the expression of ME1 as well as the glucose-6-phosphate dehydrogenase (G6PD) catalyzing the rate-limiting step of the oxidative phase of the PP pathway was significantly (q value < 0.05) upregulated in HCC. The two genes involved in the non-oxidative phase of the PP pathway, transketolase (TKT) and transaldolase 1 (TALDO1), were also significantly (q value < 0.05) upregulated in HCC. Intermediates of the PP pathway are also used as precursors for nucleotide biosynthesis, a metabolic feature essential for tumor growth, and upregulation of the PP pathway may hence serve the purpose of both providing additional NADPH as well as precursors for nucleotide biosynthesis (Figure 2).
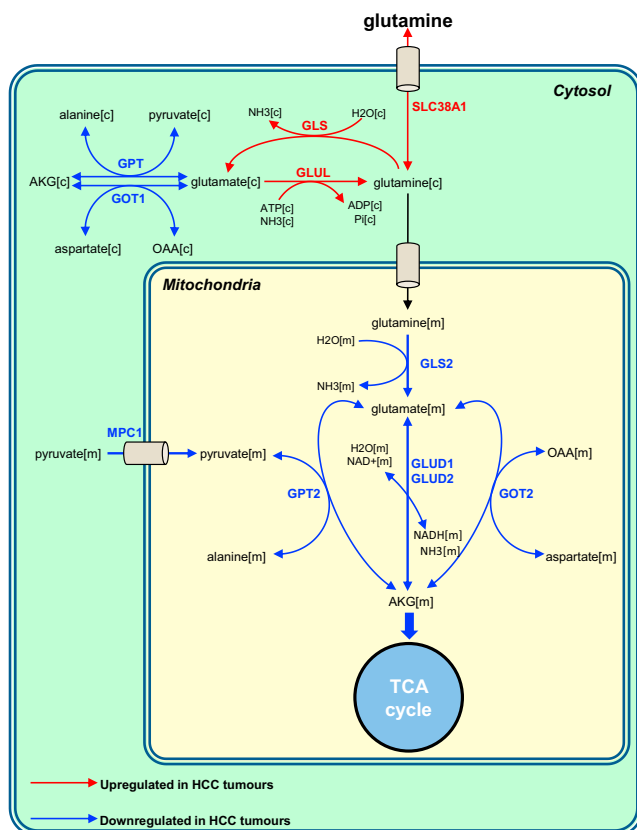
Figure 2. Major Metabolic Alterations in HCC Compared to Noncancerous Liver Samples

Fatty acid biosynthesis (FAB), the pentose phosphate (PP) pathway, and glycolysis show significant upregulation, whereas FAB showed significant tight regulation in HCC. Fatty acid oxidation and gluconeogenesis display significant downregulation in HCC. DIRAC analysis pointed out to significant deregulation of the TCA cycle and the electron transport chain in HCC patients. Generation of acetyl-CoA from acetate by ACSS1 in the mitochondria significantly upregulated in HCC, and mitochondrial acetate is used as a metabolic fuel for the growth and proliferation of tumors. Arrows are colored, based on the direction of change in the expression of the corresponding genes associated to the reaction. Blue arrows indicate significant (q value < 0.05) downregulation, whereas red arrows indicate significant (q value < 0.05) upregulation of the associated genes. The detailed descriptions of the genes and the metabolites are included in the SBML model file. See also Figures S2 and S3 and Data S1.

De novo synthesized FAs can be incorporated into lipid droplets (LDs), the intracellular reservoir of neutral fat, and very low density lipoproteins (VLDLs) that are exporting neutral fat. We examined the expression of the genes involved in the formation of the LDs and VLDLs. Among these genes, perilipins (PLIN1 and PLIN2) and patatin-like phospholipase domain-containing proteins (PNPLA4, PNPLA7, and PNPLA8) involved in LD formation as well as microsomal triglyceride transfer protein large subunit (MTTP), APOB protein, and transmembrane 6 superfamily member 2 (TM6SF2) involved in VLDLs secretion were downregulated in HCC patients (Data S1E). Of note, human naturally occurring mutations in the PNPLA3 and TM6SF2 proteins confer a robust susceptibility to chronic liver disease progression (Dongiovanni et al., 2013, 2014). Taken together, our results indicated funda-

mental changes in fatty acid metabolism of HCC with induction of FAB that has been linked to tumor growth and proliferation.

Mitochondrial Alterations in HCC

In contrast to FAB, DIRAC analysis revealed highly significant deregulation of mitochondrial β-oxidation in HCC pointing to large variation in expression of genes associated with these pathways in HCC patients. The majority of genes involved in FAO including the acyl-CoA dehydrogenase family (e.g., ACADSB), the acetyl-CoA acyltransferases (ACAA1 and ACAA2), and the hydroxyacyl-CoA dehydrogenases (HADH, HADHA, and HADHB) were significantly (q value < 0.05) downregulated in HCC tumors (Data S1G). In addition, carnitine palmitoyltransferase 2 (CPT2) that is responsible for the translocation of fatty

Figure 3. Decreased Expressions of Genes Involved in Glutamate Utilization in HCC

Glutamine is not used to fuel growth and proliferation of tumors in HCC tumors. Even though glutamine uptake is increased in HCC through significant (q value < 0.05) upregulation of SLC38A1, the expression of the enzymes catalyzing the subsequent conversion of glutamate to α-ketoglutarate (AKG) in mitochondria and cytosol are significantly (q value < 0.05) downregulated. Blue arrows indicate significant (q value < 0.05) downregulation, whereas red arrows indicate significant (q value < 0.05) upregulation of the associated genes.

acyl-CoA esters from the cytosol to the mitochondria was significantly (q value < 0.05) downregulated. Further on, DE analysis revealed FAO as one of the pathways with the highest degree of downregulation in HCC.

The DIRAC analysis also revealed the TCA cycle and the electron transport chain (ETC) as two of the pathways with highest degree of deregulation in HCC. Interestingly, the majority of the genes in the TCA cycle displayed no differential expression, thus the DIRAC algorithm detected possible dysfunction of the TCA cycle not obviously related to upregulation or downregulation of the enzymes. Significant downregulation of succinate dehydrogenase genes (SDHA, SDHB, and SDHD) also displayed dysfunction of the ETC both in terms of deregulation and downregulation (Data S1G).

Pyruvate connects glycolysis to the TCA cycle and it is transported from cytosol to the mitochondria with the mitochondrial pyruvate carrier proteins (MPC1 and MPC2) (Herzig et al., 2012). Loss of either MPC1 or MPC2 results in defective pyruvate

carrier activity thus suggesting both genes are needed to form a functioning carrier protein (Herzig et al., 2012). We found that MPC1 was significantly (q value < 0.05) downregulated in HCC tumors. With the loss of MPC activity in HCC, pyruvate would not be able to enter the mitochondria and thus inhibit oxidative phosphorylation of pyruvate, even in the presence of oxygen. MPC also provides an important link between glycolysis and gluconeogenesis since pyruvate entering the mitochondria is the end point of glycolysis and the starting point of gluconeogenesis. As in the Warburg effect, some of the glycolytic genes showed significant upregulation in HCC, whereas gluconeogenesis displayed downregulation and apparent dysfunction (Data S1G). The first step in gluconeogenesis is the conversion of oxaloacetate (OAA) to phosphoenolpyruvate (PEP). This reaction is catalyzed by the enzyme phosphoenolpyruvate carboxykinases, PCK1 and PCK2, that were significantly downregulated in HCC. The conversion of fructose 1,6-bisphosphate to fructose 6-phosphate catalyzed by the enzyme fructose-1,6-bisphosphatase 1 (FBP1) that constitutes a key regulatory step in gluconeogenesis was also significantly downregulated in HCC.

Repression of the MPC could, however, be offset by glutamine-based anaplerosis of the TCA cycle. Glutamine metabolism also displayed alterations in HCC (Figure 3), with apparent high uptake of glutamine through upregulation of sodium-coupled neutral amino acid transporter 1 (SLC38A1) but suppressed conversion of glutamate to α-ketoglutarate (AKG) through downregulation of glutamate dehydrogenases (GLUD1 and GLUD2), glutamic-oxaloacetic transaminases (GOT1 and GOT2), and glutamic-pyruvate transaminases (GPT1 and GPT2) (Figure 4A). Our results indicated that glutamine carbon may not actively oxidize in the TCA cycle in HCC tumors based on the expression of the genes utilizing glutamine, and this behavior differs from the proposed role of glutamine as an anaplerotic substrate for the TCA cycle in certain cancers (Le et al., 2012; Metallo et al., 2012; Mullen et al., 2012).

Mitochondrial Acetate Is Predicted as a Substrate in FAB

In mammalian cells, the acetyl-CoA used for FAB and histone acetylation is primarily supplied by mitochondria-derived citrate (Wellen et al., 2009). Mitochondrial acetyl-CoA is generally produced by the degradation of lipids and proteins or the conversion of pyruvate to acetyl-CoA in the mitochondria. Our analysis revealed deregulation and downregulation of β-oxidation as well as attenuation of MPC function in HCC. In addition, the potential incorporation of glutamine to citrate via anaplerosis of the TCA cycle was downregulated in HCC. Therefore, the main source of mitochondrial acetyl-CoA did not result from any of these pathways in HCC.

We predicted mitochondrial acetate as an alternative substrate for FAB in HCC tumors based on the expression of the genes. Acetate can be converted to acetyl-CoA by mitochondrial ACSS1 and ACSS3 or cytosolic ACSS2 (Figure 2). The expression of ACSS1 was significantly upregulated in HCC compared to noncancerous liver (Figure 5A). In contrast, we did not detect any significant changes in the expression of ACSS2 nor ACSS3 between HCC and noncancerous liver samples (Figure 5A). The mRNA expression of the ACSS1 and ACSS2 has also been
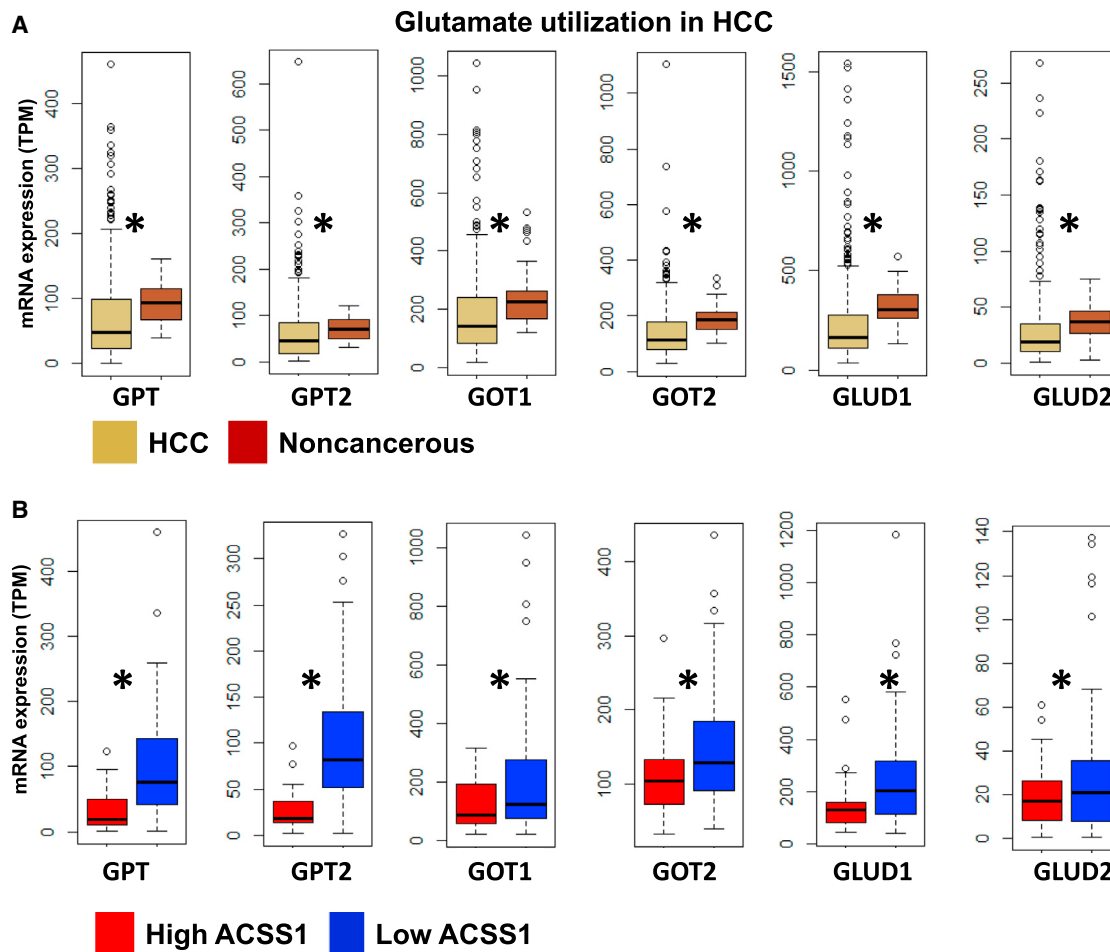
Figure 4. Expressions of the Enzymes Involved in Glutamate Utilization in HCC Patients
mRNA expression of the enzymes involved in the conversion of glutamate to α-ketoglutarate (AKG) including GPT, GPT2, GOT1, GOT2, GLUD1, and GLUD2 are shown in (A) HCC patients and noncancerous liver samples as well as (B) in HCC patients stratified by high and low ACSS1 expression. (*q value < 0.05). See also Figures S4 and S5 and Data S1.

measured in healthy liver as well as other major human tissues, and it has been shown that ACSS1 has low, whereas ACSS2 has high, expression in the healthy liver tissue (Kampf et al., 2014a; Uhlén et al., 2015).

We also investigated the differences in the expression of the genes catalyzing production of acetate within HCC tumors to detect a possible source of acetate within the HCC tumors. We did not detect any changes in the expression of genes that produce acetate in HCC (Data S1G). Hence, we hypothesized that the acetate potentially used by HCC tumors may be taken up from the plasma of the subjects.

Stratification of HCC Patients Based on the Expression of ACSS1

We found significant upregulation of ACSS1, but neither ACSS2 nor ACSS3 in HCC compared to noncancerous liver samples (Figure 5A). However, upon closer inspection, we observed that the expression of ACSS1 varied substantially between HCC patients. Therefore, we compared the global gene expres-

sion profiling of the HCC tumors in the top tenth percentile with highest expression of ACSS1 (n = 36) with the quartile of HCC tumors (n = 90) with the lowest expression of ACSS1 to understand its key role in cancer progression. The average expression of the top tenth percentile was 35.1 transcripts per million (TPM) compared to the lowest quartile with average expression of 1.0 TPM (Figure 5B). The top tenth percentile was selected as these tumors clearly displayed ACSS1 expression values far above the normal range, whereas the lowest quartile was selected because of the very low expression of ACSS1, yet relatively large sample size.

DE analysis revealed 3,814 genes (Data S1H) being significantly (q value < 0.05) differentially expressed between these groups, indicating substantial differences between HCC tumors stratified by high and low ACSS1 expression. Such large heterogeneity in gene expression in HCC is consistent with our earlier study on HCC (Agren et al., 2014). It should be noted that we did not detect any significant differences in the expression of ACSS2 within these patients (Figure 5B). We performed GSA
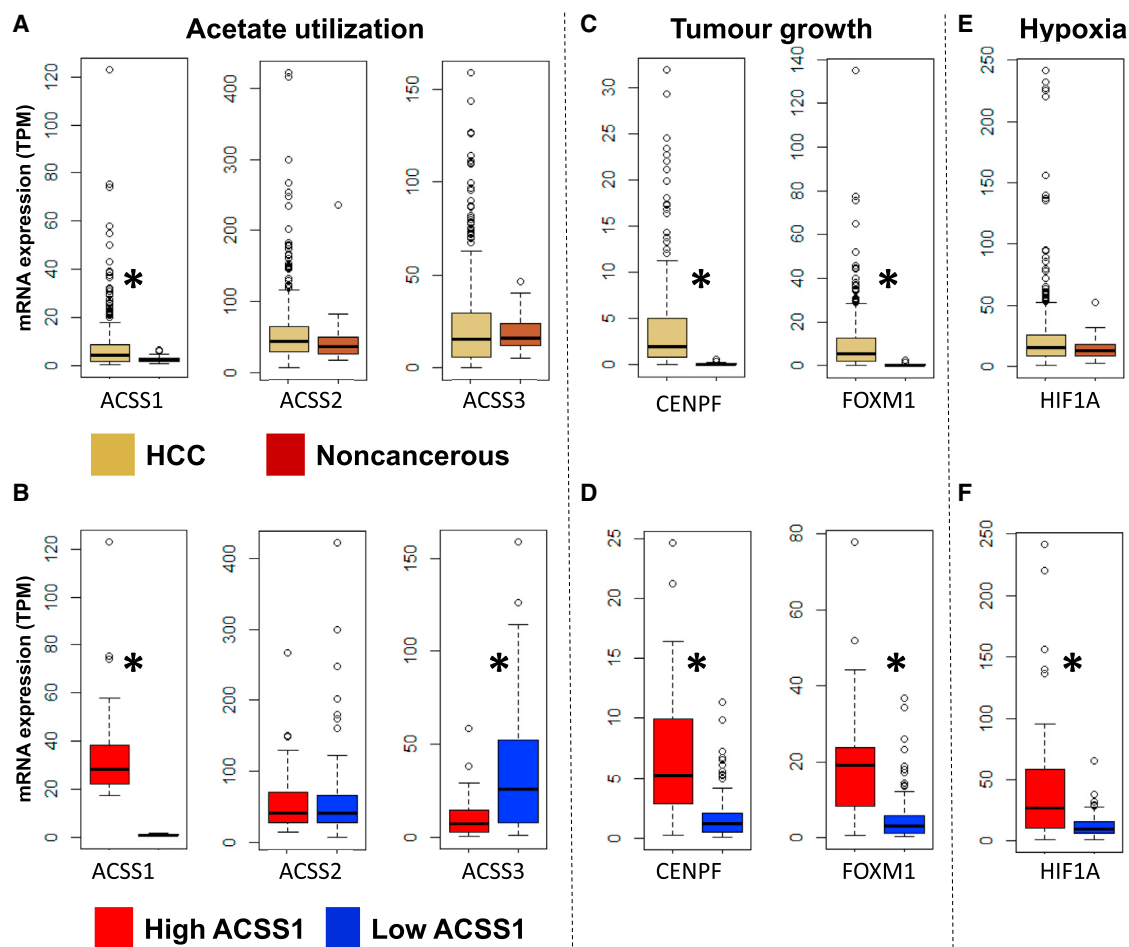
Figure 5. Mitochondrial Acetate Supports Tumor Growth under Hypoxia
mRNA expression of the ACSS1, ACSS2, and ACSS3, converting acetate to acetyl-CoA (A and B), CENPF, FOXM1, indicating aggressive HCC tumor growth (C and D), and HIF1A (E and F). A tell-tale sign of hypoxia is shown in HCC patients and noncancerous liver samples as well as in HCC patients stratified by high and low ACSS1 expression, respectively (*q value < 0.05).
See also Figures S4 and S5 and Data S1.

between the high and low ACSS1-expressing HCC patients based on GO BP terms and revealed biological processes related to cell proliferation being associated with upregulated genes and major catabolic processes being associated with the downregulated genes (Figure S4). We also identified oxygen as one of the top reporter metabolites associated with down-regulated genes in HCC patients with high ACSS1 expression compared to low ACSS1 expression (Figure S5; Data S1I). Hence, we predicted that increased expression of ACSS1 is associated with repression of oxygen-consuming reactions in the HCC tumor microenvironment based on gene expression data.

We further investigated if any of the derangements in central metabolic pathways between HCC and noncancerous liver were also present between HCC patients stratified by high and low ACSS1 expression. The majority of the genes involved in FAO were significantly downregulated in tumors with high ACSS1 expression compared to low ACSS1 expression (Data

S1G). In addition, GSA revealed FAO as significantly downre-gulated. This indicated that the clear general suppression of FAO found in HCC is further exacerbated in patients with high ACSS1 expression possibly due to the limited oxygen as is often seen in the microenvironment of a tumor.

The enzyme pyruvate kinase (PKM) was significantly (q value < 0.05) upregulated in HCC patients with high ACSS1 expression. We found that expression of PKM was increased ∼4-fold in HCC compared to noncancerous liver and further increased 5-fold in patients with high ACSS1 expression. Upregulation of PKM may result in increased ability of metabolic adaptation to varying nutrient and oxygen concentrations. The isoform PFKP of the enzyme catalyzing the committed step of glycolysis was also significantly (q value < 0.05) upregulated in patients with high ACSS1 expression supporting further increased glycolytic flux in these patients. On the other hand, PCK1 and PCK2 involved in gluconeogenesis were downregulated, indicating further sup-pression of this pathway (Data S1G).

We also found that all genes involved in glutaminolysis and glutamate utilization were significantly downregulated in patients with high ACSS1 expression compared to low ACSS1 expression (Figure 4B). For instance, the expression of GPT2 was further suppressed in HCC patients with high ACSS1 expression and decreased ~5-fold, whereas its expression decreased 2-fold in HCC tumors compared to noncancerous liver samples.

Tumor Growth under Hypoxic Condition Is Associated with Increased ACSS1 Expression

GO BP terms including cell proliferation, regulation of cell proliferation, positive regulation of cell proliferation, cell-cycle process, system development, and organ development are associated with upregulated genes in HCC patients with high ACSS1 expression (Figure S4). We also investigated the changes in the expression of transcription factor forkhead box M1 (FOXM1) and centromere protein F (CENPF). CENPF is involved in mitosis, and its increased expression was positively correlated with venous invasion, advanced differentiation stage, and a shorter overall survival in HCC patients (Dai et al., 2013). FOXM1 has been shown to be a proliferation-specific transcription factor related to HCC cell growth (Luo et al., 2014). CENPF and FOXM1, which were two of the most significantly upregulated genes in HCC compared to noncancerous liver (Figure 5D), were further upregulated in tumors with high expression of ACSS1 (Figure 5C). Thus, increased expression of FOXM1 and CENPF may likely serve as an indicator of active proliferation in patients with high ACSS1 expression.

The above metabolic alterations in HCC patients with high expression of ACSS1, particularly suppression of FAO and increased PKM, have previously been related to hypoxia and increased de-differentiation of HCC tumors (Tanaka et al., 2013). Increased de-differentiation is a sign of malignancy, increased growth rate, and invasiveness of a tumor. These features have, in turn, been related to hypoxia, likely because a rapidly growing tumor outgrows vasculature and thus induces a hypoxic environment. A tell-tale sign of hypoxia is increased expression of hypoxia-inducible factor 1 α (HIF1A). Indeed, HIF1A was significantly (q value < 0.5) upregulated in HCC patients with high ACSS1 expression compared to low ACSS1 (Figure 5F). Interestingly, HIF1A was not differentially expressed between HCC and noncancerous liver (Figure 5E). This may indicate that oxygen tension varies between HCC patients and is related to expression of ACSS1 as well as other metabolic alterations observed between patients with high and low expression of ACSS1. Cancer proliferates and activates a hypoxic response program that comprises enhanced glycolysis, reduced glucose entry into the TCA cycle, and upregulation of glutaminolysis. However, we found that glutamate utilization was also downregulated in HCC patients with high ACSS1 expression, and acetate in the mitochondria was likely to contribute to citrate and lipogenic acetyl-CoA under hypoxic conditions.

Moreover, we calculated pairwise Spearman correlation coefficients (r) between the mRNA expressions of the ACSS1, FOXM1, CENPF, and HIF1A in HCC tumors. We found that the expression of ACSS1 significantly (p value < 0.001) positively correlated with the expression of the FOXM1, CENPF, and HIF1A (r = 0.38, 0.37, and 0.39, respectively).

Stratification of HCC Patients Based on the Expression of ACSS2

We also stratified the HCC patients based on the expression of ACSS2 to understand its critical role in the development of HCC tumors. We compared the global gene expression profiling of the HCC tumors in the top tenth percentile with the highest expression of ACSS2 (n = 36) with the quartile of HCC tumors (n = 90) having the lowest expression of ACSS2 and identified only 255 significantly (q value < 0.05) differentially expressed between these groups (Data S1J). Our analysis displayed minor biological differences between HCC patients stratified based on the expression of ACSS2 compared to patients stratified by the expression of ACSS1.

We performed GSA based on GO BP terms and found that cell proliferation, regulation of cell proliferation, system development, and mitosis were associated with downregulated genes. Fatty acid biosynthetic and metabolic process, steroid biosynthetic process, bile acid metabolic process, and other biosynthetic processes were associated with upregulated genes in patients with high ACSS2 expression (Figure S6). GO BP terms (i.e., cell proliferation and regulation of cell proliferation) associated with downregulated genes in HCC patients with high ACSS2 expression were identified as GO BP terms associated with upregulated genes in HCC patients with high ACSS1 expression. We also identified reporter metabolites and found that oxygen and other metabolites involved in steroid, arachidonate, leukotriene, and bile acid metabolism were associated with upregulated genes, and metabolites involved in glycosphingolipid metabolism were associated with downregulated genes (Figure S7; Data S1K). It should be noted that reporter metabolites (i.e., oxygen, estrone, testosterone, and arachidonate) associated with upregulated genes in HCC patients with high ACSS2 expression were also identified as reporter metabolites in HCC patients with high ACSS1 expression but associated with downregulated genes (Figure S5).

We found that FASN was significantly upregulated in HCC patients with high ACSS2 expression (Data S1G). Interestingly, we also found that ACADL, ACOX2, and EHHADH involved in FAO were significantly upregulated in patients with high ACSS2 expression that was a complete opposite phenotype in patients with high ACSS1 expression. Moreover, PCK2 involved in gluconeogenesis was upregulated, and there were no transcriptional changes in glycolysis in HCC patients with high ACSS2 expression. Hence, we observed that acetyl-CoA produced by the FAO may be used as a substrate for FAB in patients with high ACSS2 expression based on gene expression data.

We found that none of these genes involved in glutamine utilization including GLUD1, GLUD2, GOT1, GOT2, GPT1, and GPT2 were significantly differentially expressed between the HCC patients with high and low ACSS2 expression indicating that the increased expression of ACSS2 has no effect on the utilization of the glutamine (Data S1G). We finally calculated pairwise Spearman correlation coefficients between the expression of the ACSS2, FOXM1, CENPF, and HIF1A in HCC tumors. We found that the expression of ACSS2 was not correlated with the expression of the FOXM1 and CENPF (p value = 0.35 and 0.45, respectively) and significantly (p value < 0.01) negatively correlated with the expression of the HIF1A (r = −0.16).
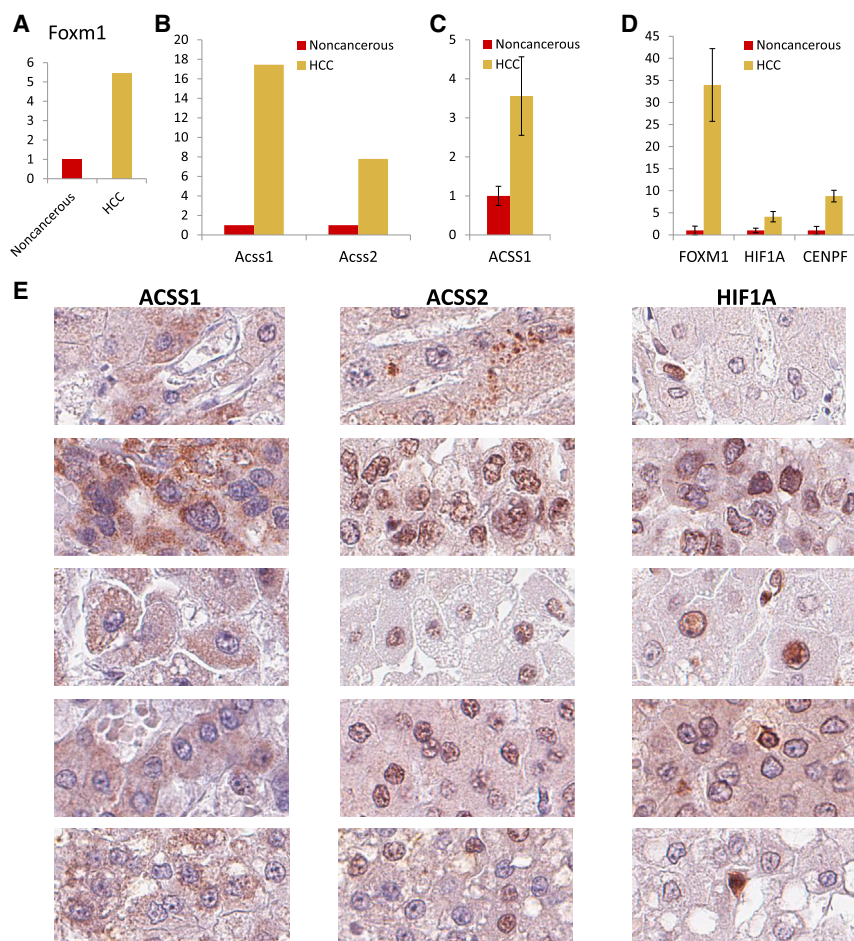
Figure 6. Induction of ACSS1 in Murine and Human HCC Samples

(A–D) mRNA expression of the Foxm1 (A), Acss1, and Acss2 (B) is measured in six pooled wild-type HCC tumor and noncancerous samples using RNA-seq. The mRNA expression of the ACSS1 (C) as well as the FOXM1, HIF1A, and CENPF (D) is measured using RNA-seq in tumor and noncancerous liver samples obtained from four independent HCC patients.

(E) Immunohistochemical staining of the proteins (ACSS1, ACSS2, HIF1A) in five human HCC tumors are presented. Protein expression is seen in brown, counterstaining in blue.

Induction of ACSS1 in Murine and Human HCC Samples

Endocannabinoids acting on hepatic cannabinoid receptor-1 (CB$_1$R) promote de novo lipogenesis (Osei-Hyiaman et al., 2005) and inhibit FAO in the liver (Osei-Hyiaman et al., 2008). Once CB$_1$R$^{+/+}$ and CB$_1$R$^{-/-}$ littermates in C57BL/6J background were injected with 25 mg/kg of DEN (Sigma) at 2 weeks after birth, the presence of the HCC tumor was verified, and its size was measured with MRI in each DEN-treated mouse 8 months after the DEN administration (Mukhopadhyay et al., 2015). Importantly, activation of hepatic CB$_1$R also promotes the initiation and progression of chemically induced HCC in mice, in which CB$_1$R were found to be overexpressed in tumor versus non-tumor tissue (Mukhopadhyay et al., 2015). The expression of FoxM1 was significantly (p value < 0.05) increased 5.4-fold in wild-type HCC tumor compared to noncancerous samples obtained from CB$_1$R$^{+/+}$ mice (Figure 6A). Moreover, nuclear localization of FoxM1 was observed in HCC tumor samples obtained from CB$_1$R$^{+/+}$ mice.

Interestingly, the expression of CNR1, the gene encoding the human CB$_1$R, was significantly increased 6.5-fold (q value < 0.05) in HCC tumors compared to noncancerous liver samples. Moreover, the expression of the CNR1 was significantly increased 3.7-fold (q value < 0.05) in HCC tumors with high ACSS1 compared to low ACSS1 expression, whereas its expres-

sion was not changed between the tumors with high and low ACSS2. Because of these intriguing parallels, we retrospectively analyzed the mRNA expression levels of Acss1 and Acss2 in the HCC and noncancerous liver samples obtained from wild-type and CB$_1$R$^{-/-}$ mice (Mukhopadhyay et al., 2015). We found that the expression of Acss1 is increased 17.5-fold, whereas the expression of the Acss2 is increased 7.8-fold in a pooled wild-type HCC tumor compared to noncancerous samples (Figure 6B), and the expression in CB$_1$R$^{-/-}$ mice was at or below the detection limit both in HCC and adjacent noncancerous samples.

We measured the mRNA expression of the ACSS1 in four independent human HCC tumor samples and adjacent noncancerous liver samples (Mukhopadhyay et al., 2015) and found that its expression was increased 3.6-fold in human HCC tumors (Figure 6C). The expressions of FOXM1, HIF1A, and CENPF were also increased 34-fold, 4.1-fold, and 8.8-fold, respectively, in these human HCC samples (Figure 6D). Moreover, we analyzed protein expression level of ACSS1, ACSS2, and HIF1A using the antibodies generated in the HPA project including HPA041014, HPA004141, and HPA001275, respectively, (Uhlén et al., 2010, 2015) in five additional independent human HCC tumor samples. We observed that ACSS1 had moderate/strong protein expression levels in the mitochondria, whereas ACSS2 had none/low protein expression level in the cytosol. Moreover, we found that HIF1A had moderate/strong protein expression levels in HCC tumors. Protein expression levels in HCC tumors as detected by using immunohistochemistry (IHC) are presented in Figure 6E.

DISCUSSION

We demonstrated that HCC tumors may have completely opposite metabolic programming, and stratification of HCC patients is highly desirable for development of effective treatment strategies. In this context, we analyzed the global gene expression profiling of HCC and noncancerous liver using DE and
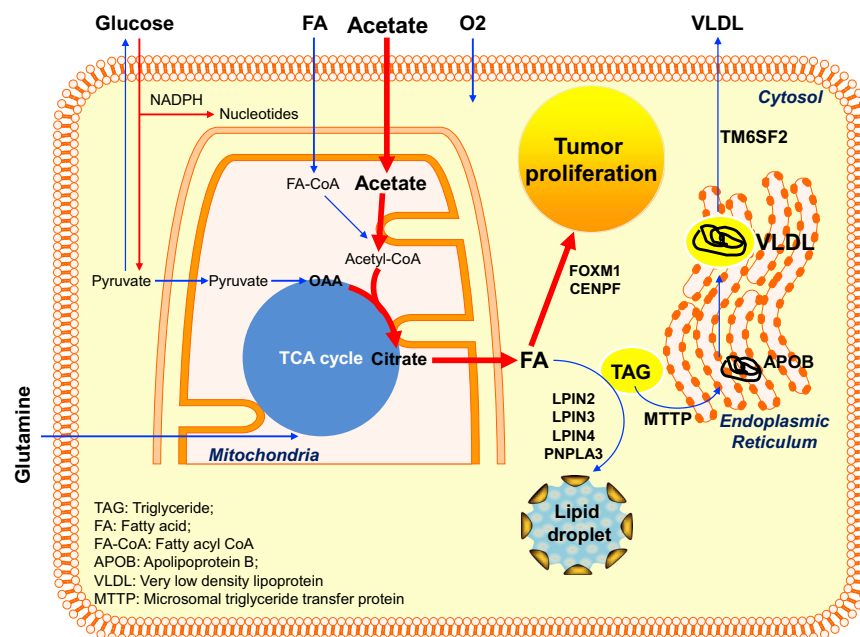
Figure 7. Pathophysiology of HCC with High ACSS1 Expression

Mitochondrial acetate is used to fuel the fatty acid biosynthesis (FAB) that is required for HCC tumor growth and proliferation under hypoxic conditions. The amount of the fatty acids (FAs) stored in the lipid droplets (LDs) as well as FAs incorporated into very low density lipoproteins (VLDLs) are decreased in HCC tumors.

used as a substrate for FAB. The treatment of prostate cancer cells with a FASN inhibitor resulted in reduced acetate uptake, thus there is a clear association between FASN expression and acetate uptake (Vävere et al., 2008). Based on the associations between high acetate uptake and increased cell growth and/or malignancy of HCC, we predicted that acetate uptake may cause more glucose-derived carbon to be available for macromolecular biosynthesis and histone modification. This may result in two phenomena: growth when glucose is limited and a more rapid growth when glucose is abundant. In other words, acetate as an extra carbon source would serve to relieve the demand for glucose-derived carbons for lipid production.

We presented the pathophysiology of HCC tumors with high ACSS1 expression in Figure 7. Our study highlighted the possible role of mitochondrial acetate as a carbon source for lipid production in HCC. If FOXM1 and CENPF are drivers of malignancy in HCC, a connection between high ACSS1 expression and increased growth and malignancy exists. Further on, significant positive correlation between increased ACSS1 expression and HIF1A is obtained from our analyses. Indeed, we predicted that high acetate uptake may result in increased cell growth and/or malignancy of HCC under hypoxic conditions. Acetate uptake in cancer cell lines also increase when subjected to hypoxia (Yoshii et al., 2009), and radiolabeled glucose and acetate showed a complementary uptake pattern in HCC patients in vivo (Yun et al., 2009). These two observations indicate a heterogeneous uptake of glucose and acetate within the same tumor. Taken together with the results of the present study, this could indicate that there is clear association between increased tumor growth, malignancy, hypoxia, and acetate uptake between different HCC patients but also between different parts of the same tumor.

Previously, Yun et al. (2009) observed that ACSS1 was highly expressed in SNU 449 cells (human HCC cell lines from the Korean Cell Line Bank) with high uptake of labeled acetate uptake and suggested the use of mitochondrial acetyl CoA for lipid synthesis. In order to show the effect of ACSS1 on acetate uptake and cell viability, the authors inhibited ACSS1 using corresponding small interfering RNA (siRNA) in SNU 449 cells. Hereby, they found that the amount of acetate uptake and viability of the cells was reduced more in wells with ACSS1 siRNA than in the well with a control siRNA.

DIRAC analysis based on the network topology provided by *iHCC2578*. Reported metabolic alterations in HCC conspired to a metabolic phenotype supporting cell growth with induction of FAB for production of cell membrane material, high glycolytic flux providing glycolytic intermediates for additional macromolecular biosynthesis, and production of growth-supporting NADPH. We observed significant downregulation of gluconeogenesis as well as highly significant deregulation of the FAO, glutamate utilization, TCA cycle, and ETC in HCC tumors we have analyzed.

Previously, the targetable metabolic vulnerability of ACSS2 has been proposed in a wide spectrum of tumors, including liver cancer, in several studies (Comerford et al., 2014; Mashimo et al., 2014; Schug et al., 2015). However, the expression of ACSS2 is equally expressed both in HCC tumors and noncancerous liver samples and showed no differential expression in human HCC tumors. In contrast, we found that the expression of ACSS1 is significantly upregulated in HCC, which suggests an increased generation of acetyl-CoA from acetate in the mitochondria. Mitochondrial acetate emerged as a possible substrate for the increased FAB and had a major role in the growth and proliferation of HCC tumor.

To identify the role of ACSS1 in the development of HCC, we stratified the HCC patients based on the level of ACSS1 expression and identified the metabolic differences between these patients. We predicted that the expression of ACSS1 is associated with increased tumor growth and malignancy of HCC under hypoxic conditions. We also demonstrated increased mRNA expression of ACSS1 in murine and independent human HCC samples compared to adjacent noncancerous liver samples as well as the strong/moderate protein expression of the ACSS1 and HIF1A in additional independent human HCC samples.

Radiolabeled acetate is incorporated into the lipid soluble fraction of cancer cells (Yoshimoto et al., 2001), and acetate is

In line with our earlier study on HCC (Agren et al., 2014), we find that there is a large heterogeneity in the metabolism of HCC. Upregulation of ACSS1 or ACSS2 is consistent in the majority of the HCC patients studied here, but still the level of upregulation varies, and this allows for stratification of the subjects based on ACSS1 or ACSS2 gene expression. This again points to the importance of stratification of HCC patients and that there may only be a few targets that consistently prevent tumor growth.

The findings in the liver of wild-type mice with chemically induced HCC are similar to those in the human HCC tumor compared to noncancerous liver, and the marked overexpression of FOXM1 in human HCC is also similar to that reported earlier for mouse HCC (Mukhopadhyay et al., 2015). This parallel is further extended by the similar marked upregulation of *CNR1* in HCC tissue in both species. It is tempting to speculate that the metabolic phenotype of human HCC established in the present study is functionally linked to increased CB_1R activity. Such a hypothesis is supported by the data from $CB_1R^{-/-}$ mice in which the absence of CB_1R was associated with the absence of a detectable upregulation of lipogenic gene expression. This, and the reduced rate of tumor initiation and growth in $CB_1R^{-/-}$ mice, could warrant exploring the possible use of CB_1R antagonists as part of the pharmacotherapy of HCC. Although currently there are no CB_1R antagonists available for human use following the withdrawal of rimonabant due to neuropsychiatric side effects (Le Foll et al., 2009), non-brain-penetrant CB_1R antagonists with therapeutic efficacy via peripheral CB_1R blockade are currently being developed (Cinar et al., 2014; Tam et al., 2012).

In conclusion, we studied the individual variations in acetate utilization between HCC tumors and shed light on the molecular and cellular mechanisms underlying HCC using a systems biology approach. Expression of ACSS1 clearly correlated with substantial alterations of the HCC transcriptome as indicated by the large number of significantly differentially expressed genes between HCC patients stratified by high and low ACSS1 expression. We predicted that metabolic alterations related to high ACSS1 expression in HCC patients, (e.g., decreased FAO, glutamine utilization, gluconeogenesis, and increased glycolysis) are symptoms of an underlying increased growth under hypoxic conditions. We suggest that inhibition of ACSS1 together with ACSS2 may be used in development of effective treatment strategies for HCC patients. Lastly, the results of our systems-level analysis may open novel avenues for understanding the mechanism underlying HCC and may be used in developing potential treatments.

EXPERIMENTAL PROCEDURES

Reconstruction of the Functional GEM for HCC, *iHCC2578*

We reconstructed a functional GEM for HCC tumors, *iHCC2578* that covers the individual metabolic variations between all HCC patients. The model was reconstructed based on the proteome and transcriptome of HCC through the use of largest generic human model, Human Metabolic Reaction database 2 (HMR2) (Mardinoglu et al., 2014) and tINIT algorithm (Agren et al., 2014). Common biological tasks known to occur in all human cells as well as the growth as an additional task were used as an input to tINIT algorithm to ensure the functionality of the model. The tINIT reconstructed model was manually evaluated, and the final model was tested to see if it could successfully perform the known metabolic functions in HCC. For instance, non-essential

fatty acids and amino acids can be synthesized in the model and used as substrate for the tumor growth. *iHCC2578* is publically available in the Systems Biology Mark-up Language (SBML) format as well as in mat file format at Human Metabolic Atlas (http://www.metabolicatlas.org).

Differential Expression Analysis

RNA-seqV2 gene expression data from 361 HCC samples and 49 adjacent noncancerous liver samples were downloaded from the TCGA using the TCGA-assembler R package (Zhu et al., 2014). The analysis of RNA-seq data was performed using the differential expression sequencing (DESeq) R-package (Anders and Huber, 2010). Normalization and variance estimation was performed according to the DESeq manual before subsequent DE analysis. P values were adjusted for multiple-testing with the procedure of Benjamini and Hochberg to calculate q values, and 5,946 genes (of ~20,530) were found to be significantly differentially expressed at a false discovery rate (FDR) of 5% (q value < 0.05) between HCC and noncancerous liver samples. DE analysis revealed 3,814 and 255 genes being significantly (q value < 0.05) differentially expressed between the HCC patients stratified by high and low ACSS1 and ACSS2 expression, respectively.

The DIRAC Algorithm

The DIRAC analysis is a network-based approach, but it is specifically designed to take into account the combinatorial nature of gene interactions within the network (Eddy et al., 2010). DIRAC provides quantitative measuring of how network rankings differ among networks for a given phenotype or among phenotypes for a given network (e.g., differences in the pathways of a given GEM) based on the transcriptome of individuals (Figure S1). The network was defined as being (tightly/loosely) regulated based on the level of (high/low) conservation of transcript ordering in the transcriptome of individuals. However, a network can relatively be tightly regulated in one phenotype, whereas it can be loosely regulated in another phenotype, and this represents the deregulation of the given network.

mRNA Expression of ACSS1 and ACSS2 in Murine and Human HCC Samples

Total RNA was isolated from tumor area and noncancerous area of liver tissue samples obtained from six DEN-treated (HCC) $CB_1R^{+/+}$ mice and six $CB_1R^{-/-}$ mice (Mukhopadhyay et al., 2015). Total RNA was also isolated from noncancerous and tumor biopsies from four different additional human donors with HCC diagnosis without viral hepatitis. rRNA-depleted RNA, 100 ng for each sample, was treated with RNase III to generate 100- to 200-nt fragments, which were pooled and processed for RNA sequencing. All data were normalized based on housekeeping genes used by Program CLC Genomics Workbench program (version 5.1, CLC Bio). These absolute numbers were extracted from the reads, and the data were adjusted to non-HCC biopsies for each gene.

SUPPLEMENTAL INFORMATION

Supplemental Information includes Supplemental Experimental Procedures, seven figures, and one dataset and can be found with this article online at http://dx.doi.org/10.1016/j.celrep.2015.10.045.

AUTHOR CONTRIBUTIONS

E.B., A.M., S.F., and J.N. performed the analysis of clinical data. A.M. reconstructed *iHCC2578*. A.A., N.P., and M.U. reevaluated the antibody proteomics data for human HCC tumors. B.M., R.C., and G.K. measured the expression of the genes in murine and human HCC samples. A.M. conceived the project. A.M. and E.B. wrote the paper. All authors read and approved the final manuscript.

ACKNOWLEDGMENTS

REFERENCES

Agren, R., Bordel, S., Mardinoglu, A., Pornputtapong, N., Nookaew, I., and Nielsen, J. (2012). Reconstruction of genome-scale active metabolic networks for 69 human cell types and 16 cancer types using INIT. PLoS Comput. Biol. 8, e1002518.

Agren, R., Mardinoglu, A., Asplund, A., Kampf, C., Uhlen, M., and Nielsen, J. (2014). Identification of anticancer drugs for hepatocellular carcinoma through personalized genome-scale metabolic modeling. Mol. Syst. Biol. 10, 721.

Anders, S., and Huber, W. (2010). Differential expression analysis for sequence count data. Genome Biol. 11, R106.

Carracedo, A., Cantley, L.C., and Pandolfi, P.P. (2013). Cancer metabolism: fatty acid oxidation in the limelight. Nat. Rev. Cancer 13, 227–232.

Cinar, R., Godlewski, G., Liu, J., Tam, J., Jourdan, T., Mukhopadhyay, B., Harvey-White, J., and Kunos, G. (2014). Hepatic cannabinoid-1 receptors mediate diet-induced insulin resistance by increasing de novo synthesis of long-chain ceramides. Hepatology 59, 143–153.

Comerford, S.A., Huang, Z., Du, X., Wang, Y., Cai, L., Witkiewicz, A.K., Walters, H., Tantawy, M.N., Fu, A., Manning, H.C., et al. (2014). Acetate dependence of tumors. Cell 159, 1591–1602.

Dai, Y., Liu, L., Zeng, T., Zhu, Y.H., Li, J., Chen, L., Li, Y., Yuan, Y.F., Ma, S., and Guan, X.Y. (2013). Characterization of the oncogenic function of centromere protein F in hepatocellular carcinoma. Biochem. Biophys. Res. Commun. 436, 711–718.

Dongiovanni, P., Donati, B., Fares, R., Lombardi, R., Mancina, R.M., Romeo, S., and Valenti, L. (2013). PNPLA3 I148M polymorphism and progressive liver disease. World J. Gastroenterol. 19, 6969–6978.

Dongiovanni, P., Petta, S., Maglio, C., Fracanzani, A.L., Pipitone, R., Mozzi, E., Motta, B.M., Kaminska, D., Rametta, R., Grimaudo, S., et al. (2014). Transmembrane 6 superfamily member 2 gene variant disentangles nonalcoholic steatohepatitis from cardiovascular disease. Hepatology 61, 506–514.

Eddy, J.A., Hood, L., Price, N.D., and Geman, D. (2010). Identifying tightly regulated and variably expressed networks by Differential Rank Conservation (DIRAC). PLoS Comput. Biol. 6, e1000792.

European Association For The Study Of The Liver; European Organisation For Research And Treatment Of Cancer (2012). EASL-EORTC clinical practice guidelines: management of hepatocellular carcinoma. J. Hepatol. 56, 908–943.

Fagerberg, L., Hallström, B.M., Oksvold, P., Kampf, C., Djureinovic, D., Odeberg, J., Habuka, M., Tahmasebpoor, S., Danielsson, A., Edlund, K., et al. (2014). Analysis of the human tissue-specific expression by genome-wide integration of transcriptomics and antibody-based proteomics. Mol. Cell. Proteomics 13, 397–406.

Folger, O., Jerby, L., Frezza, C., Gottlieb, E., Ruppin, E., and Shlomi, T. (2011). Predicting selective drug targets in cancer through metabolic networks. Mol. Syst. Biol. 7, 501.

Gatto, F., Nookaew, I., and Nielsen, J. (2014). Chromosome 3p loss of heterozygosity is associated with a unique metabolic network in clear cell renal carcinoma. Proc. Natl. Acad. Sci. USA 111, E866–E875.

Ghaffari, P., Mardinoglu, A., Asplund, A., Shoaie, S., Kampf, C., Uhlen, M., and Nielsen, J. (2015). Identifying anti-growth factors for human cancer cell lines through genome-scale metabolic modeling. Sci. Rep. 5, 8183.

Herzig, S., Raemy, E., Montessuit, S., Veuthey, J.L., Zamboni, N., Westermann, B., Kunji, E.R., and Martinou, J.C. (2012). Identification and functional expression of the mitochondrial pyruvate carrier. Science 337, 93–96.

Kampf, C., Mardinoglu, A., Fagerberg, L., Hallström, B.M., Edlund, K., Lundberg, E., Pontén, F., Nielsen, J., and Uhlen, M. (2014a). The human liver-specific proteome defined by transcriptomics and antibody-based profiling. FASEB J. 28, 2901–2914.

Kampf, C., Mardinoglu, A., Fagerberg, L., Hallström, B.M., Danielsson, A., Nielsen, J., Pontén, F., and Uhlen, M. (2014b). Defining the human gallbladder proteome by transcriptomics and affinity proteomics. Proteomics 14, 2498–2507.

Le, A., Lane, A.N., Hamaker, M., Bose, S., Gouw, A., Barbi, J., Tsukamoto, T., Rojas, C.J., Slusher, B.S., Zhang, H., et al. (2012). Glucose-independent glutamine metabolism via TCA cycling for proliferation and survival in B cells. Cell Metab. 15, 110–121.

Le Foll, B., Gorelick, D.A., and Goldberg, S.R. (2009). The future of endocannabinoid-oriented clinical research after CB1 antagonists. Psychopharmacology (Berl.) 205, 171–174.

Lewis, N.E., and Abdel-Haleem, A.M. (2013). The evolution of genome-scale models of cancer metabolism. Front. Physiol. 4, 237.

Llovet, J.M., Ricci, S., Mazzaferro, V., Hilgard, P., Gane, E., Blanc, J.F., de Oliveira, A.C., Santoro, A., Raoul, J.L., Forner, A., et al.; SHARP Investigators Study Group (2008). Sorafenib in advanced hepatocellular carcinoma. N. Engl. J. Med. 359, 378–390.

Luo, D., Wang, Z., Wu, J., Jiang, C., and Wu, J. (2014). The role of hypoxia inducible factor-1 in hepatocellular carcinoma. BioMed Res. Int. 2014, 409272.

Mardinoglu, A., and Nielsen, J. (2012). Systems medicine and metabolic modelling. J. Intern. Med. 271, 142–154.

Mardinoglu, A., and Nielsen, J. (2015). New paradigms for metabolic modeling of human cells. Curr. Opin. Biotechnol. 34, 91–97.

Mardinoglu, A., Agren, R., Kampf, C., Asplund, A., Nookaew, I., Jacobson, P., Walley, A.J., Froguel, P., Carlsson, L.M., Uhlen, M., and Nielsen, J. (2013a). Integration of clinical data with a genome-scale metabolic model of the human adipocyte. Mol. Syst. Biol. 9, 649.

Mardinoglu, A., Gatto, F., and Nielsen, J. (2013b). Genome-scale modeling of human metabolism - a systems biology approach. Biotechnol. J. 8, 985–996.

Mardinoglu, A., Agren, R., Kampf, C., Asplund, A., Uhlen, M., and Nielsen, J. (2014). Genome-scale metabolic modelling of hepatocytes reveals serine deficiency in patients with non-alcoholic fatty liver disease. Nat. Commun. 5, 3083.

Mardinoglu, A., Heiker, J.T., Gärtner, D., Björnson, E., Schön, M.R., Flehmig, G., Klöting, N., Krohn, K., Fasshauer, M., Stumvoll, M., et al. (2015). Extensive weight loss reveals distinct gene expression changes in human subcutaneous and visceral adipose tissue. Sci. Rep. 5, 14841.

Mashimo, T., Pichumani, K., Vemireddy, V., Hatanpaa, K.J., Singh, D.K., Sirasanagandla, S., Nannepaga, S., Piccirillo, S.G., Kovacs, Z., Foong, C., et al. (2014). Acetate is a bioenergetic substrate for human glioblastoma and brain metastases. Cell 159, 1603–1614.

Metallo, C.M., Gameiro, P.A., Bell, E.L., Mattaini, K.R., Yang, J., Hiller, K., Jewell, C.M., Johnson, Z.R., Irvine, D.J., Guarente, L., et al. (2012). Reductive glutamine metabolism by IDH1 mediates lipogenesis under hypoxia. Nature 481, 380–384.

Mukhopadhyay, B., Schuebel, K., Mukhopadhyay, P., Cinar, R., Godlewski, G., Xiong, K., Mackie, K., Lizak, M., Yuan, Q., Goldman, D., and Kunos, G. (2015). Cannabinoid receptor 1 promotes hepatocellular carcinoma initiation and progression through multiple mechanisms. Hepatology 61, 1615–1626.

Mullen, A.R., Wheaton, W.W., Jin, E.S., Chen, P.H., Sullivan, L.B., Cheng, T., Yang, Y., Linehan, W.M., Chandel, N.S., and DeBerardinis, R.J. (2012). Reductive carboxylation supports growth in tumour cells with defective mitochondria. Nature 481, 385–388.

O'Brien, E.J., Monk, J.M., and Palsson, B.O. (2015). Using genome-scale models to predict biological capabilities. Cell 161, 971–987.

Oberhardt, M.A., Yizhak, K., and Ruppin, E. (2013). Metabolically re-modeling the drug pipeline. Curr. Opin. Pharmacol. 13, 778–785.

Osei-Hyiaman, D., DePetrillo, M., Pacher, P., Liu, J., Radaeva, S., Bátkai, S., Harvey-White, J., Mackie, K., Offertáler, L., Wang, L., and Kunos, G. (2005). Endocannabinoid activation at hepatic CB1 receptors stimulates fatty acid

synthesis and contributes to diet-induced obesity. J. Clin. Invest. *115*, 1298–1305.

Osei-Hyiaman, D., Liu, J., Zhou, L., Godlewski, G., Harvey-White, J., Jeong, W.I., Bátkai, S., Marsicano, G., Lutz, B., Buettner, C., and Kunos, G. (2008). Hepatic CB1 receptor is required for development of diet-induced steatosis, dyslipidemia, and insulin and leptin resistance in mice. J. Clin. Invest. *118*, 3160–3169.

Patil, K.R., and Nielsen, J. (2005). Uncovering transcriptional regulation of metabolism by using metabolic network topology. Proc. Natl. Acad. Sci. USA *102*, 2685–2689.

Schug, Z.T., Peck, B., Jones, D.T., Zhang, Q., Grosskurth, S., Alam, I.S., Goodwin, L.M., Smethurst, E., Mason, S., Blyth, K., et al. (2015). Acetyl-CoA synthetase 2 promotes acetate utilization and maintains cancer cell growth under metabolic stress. Cancer Cell *27*, 57–71.

Shoaie, S., and Nielsen, J. (2014). Elucidating the interactions between the human gut microbiota and its host through metabolic modeling. Front. Genet. *5*, 86.

Tam, J., Cinar, R., Liu, J., Godlewski, G., Wesley, D., Jourdan, T., Szanda, G., Mukhopadhyay, B., Chedester, L., Liow, J.S., et al. (2012). Peripheral cannabinoid-1 receptor inverse agonism reduces obesity by reversing leptin resistance. Cell Metab. *16*, 167–179.

Tanaka, M., Masaki, Y., Tanaka, K., Miyazaki, M., Kato, M., Sugimoto, R., Nakamura, K., Aishima, S., Shirabe, K., Nakamuta, M., et al. (2013). Reduction of fatty acid oxidation and responses to hypoxia correlate with the progression of de-differentiation in HCC. Mol. Med. Rep. *7*, 365–370.

Uhlén, M., Oksvold, P., Fagerberg, L., Lundberg, E., Jonasson, K., Forsberg, M., Zwahlen, M., Kampf, C., Wester, K., Hober, S., et al. (2010). Towards a knowledge-based Human Protein Atlas. Nat. Biotechnol. *28*, 1248–1250.

Uhlén, M., Fagerberg, L., Hallström, B.M., Lindskog, C., Oksvold, P., Mardinoglu, A., Sivertsson, Å., Kampf, C., Sjöstedt, E., Asplund, A., et al. (2015). Proteomics. Tissue-based map of the human proteome. Science *347*, 1260419.

Väremo, L., Nielsen, J., and Nookaew, I. (2013). Enriching the gene set analysis of genome-wide data by incorporating directionality of gene expression and combining statistical hypotheses and methods. Nucleic Acids Res. *41*, 4378–4391.

Väremo, L., Scheele, C., Broholm, C., Mardinoglu, A., Kampf, C., Asplund, A., Nookaew, I., Uhlén, M., Pedersen, B.K., and Nielsen, J. (2015). Proteome- and transcriptome-driven reconstruction of the human myocyte metabolic network and its use for identification of markers for diabetes. Cell Rep. *11*, 921–933.

Vāvere, A.L., Kridel, S.J., Wheeler, F.B., and Lewis, J.S. (2008). 1-11C-acetate as a PET radiopharmaceutical for imaging fatty acid synthase expression in prostate cancer. J. Nucl. Med. *49*, 327–334.

Wellen, K.E., Hatzivassiliou, G., Sachdeva, U.M., Bui, T.V., Cross, J.R., and Thompson, C.B. (2009). ATP-citrate lyase links cellular metabolism to histone acetylation. Science *324*, 1076–1080.

Yizhak, K., Gaude, E., Le Dévédec, S., Waldman, Y.Y., Stein, G.Y., van de Water, B., Frezza, C., and Ruppin, E. (2014). Phenotype-based cell-specific metabolic modeling reveals metabolic liabilities of cancer. eLife *3*, e03641.

Yizhak, K., Chaneton, B., Gottlieb, E., and Ruppin, E. (2015). Modeling cancer metabolism on a genome scale. Mol. Syst. Biol. *11*, 817.

Yoshii, Y., Waki, A., Furukawa, T., Kiyono, Y., Mori, T., Yoshii, H., Kudo, T., Okazawa, H., Welch, M.J., and Fujibayashi, Y. (2009). Tumor uptake of radiolabeled acetate reflects the expression of cytosolic acetyl-CoA synthetase: implications for the mechanism of acetate PET. Nucl. Med. Biol. *36*, 771–777.

Yoshimoto, M., Waki, A., Yonekura, Y., Sadato, N., Murata, T., Omata, N., Takahashi, N., Welch, M.J., and Fujibayashi, Y. (2001). Characterization of acetate metabolism in tumor cells in relation to cell proliferation: acetate metabolism in tumor cells. Nucl. Med. Biol. *28*, 117–122.

Yun, M., Bang, S.H., Kim, J.W., Park, J.Y., Kim, K.S., and Lee, J.D. (2009). The importance of acetyl coenzyme A synthetase for 11C-acetate uptake and cell survival in hepatocellular carcinoma. J. Nucl. Med. *50*, 1222–1228.

Zhu, Y., Qiu, P., and Ji, Y. (2014). TCGA-assembler: open-source software for retrieving and processing TCGA data. Nat. Methods *11*, 599–600.